

Risk-Mitigated Optimal Power Flow with High Wind Penetration

A. Emma Sjödin, Dennice F. Gayme and Ufuk Topcu

Abstract—Increased penetration of renewable energy sources poses new challenges for the power grid, mostly due to their inherent variability. In the presence of such variability, reliable operation of the grid will require increased amounts of ancillary services. We consider a case where wind generators are the primary energy source with energy storage and spinning reserves from conventional sources available to provide ancillary services. The problem is formulated as a risk-mitigated optimal power flow (OPF) problem, where the objective is the scheduling of spinning reserves to minimize the cost of ancillary services and a chance constraint is used as the risk-mitigating factor that compensates for uncertainties in generation and load. This OPF with energy storage dynamics is solved as a finite-horizon optimal control problem that we apply to several case studies using the topology of the IEEE 14 bus benchmark system. We then extend the framework to investigate the optimal distribution of storage capacity across different network topologies. The results of the case studies quantify the need for ancillary services and suggest a strategy for their scheduling and placement.

I. INTRODUCTION

There is a rapidly growing interest in replacing fossil fuel based power generation with renewable energy sources. These sources are desirable, not only for being more ecologically sustainable, but also due to increasing fossil fuel prices caused by diminishing supplies [1]. The integration of renewables to the power grid is currently being accelerated through a number of government mandates [2] and incentives aimed at making the electricity grid "greener". Grid integration can take place both at the transmission level, with mainly large wind farms or solar power installations, or at distribution level, typically with residential photovoltaic panel installations. In either case, a high penetration of solar or wind power poses a number of challenges primarily due to the intermittent availability of such sources. It is widely accepted that substantial changes to the power grid will be needed for penetration levels above 20% [3], [4], [5]. One of the key strategies to address these challenges is to introduce large-scale energy storage to the grid. When used effectively, these storage systems can minimize the amounts of spilled energy [4], [5], [6], [7] as well as provide high quality ancillary services and increase transmission capacity [8].

The role of energy storage in power systems has been extensively investigated. An early simulation study in 1981 [9] confirmed the benefits of quickly dispatchable batteries for peak-shaving and power regulation. More recently, [10], [11] and [12] have studied the extent to which grid integrated

storage can address the challenges posed by renewable energy sources. One important question that arises in moving toward a power system with large-scale energy storage is how to distribute the storage capacity across the network. Although this problem was addressed in [8] and [13], the studies did not include analysis within an optimal power flow setting. In addition, most of the existing literature lacks temporal analysis. Given the variability in time that is characteristic to many renewable energy sources, and the fact that storage systems reduce the requirement for instantaneous power balance, temporal analysis covering the entire operating time line is critical. Specifically, such studies are necessary to evaluate the types of new, more flexible, grid operating paradigms that will be needed to deal with a high penetration of wind power, which is highly random and can not be controlled in the same way as conventional generators [14], [8], [15].

The power industry with mainly conventional generation has dealt with potential failures due to random events such as line or generator failures using deterministic, worst-case dispatch [4]. In this strategy the system operator schedules generation according to the *N-1 contingency criterion*, according to which all *N* possible *contingencies*, i.e. failures or outages of lines or generators, are gone through, allocating reserves to meet operating criteria in all possible cases of only *N-1* functioning units. This conservative strategy for the planning of reserves has thus far also successfully accounted for any load variability [16]. However, if these deterministic criteria for the allocation of reserves are directly applied to renewable energy sources with their high level of uncertainty, a large amount of operating reserves provided by conventional generators will be needed and the potential benefits in terms of reductions in green house gas emissions may be overshadowed [4].

The need for new operating criteria has led to considerable research activity. For example, the authors of [15] compare the *N-1 contingency criterion* to other operating criteria based on generation and load variability. Partly probabilistic operating criteria, including e.g. the *loss-of-load probability* (LOLP), were introduced in the market clearing algorithm of [16] and the concept of stochastic security was developed further in [17]. The authors of [4] propose a risk-limiting dispatch formulation that limits the LOLP using real-time information about generation and loads, which they presume will be available in a "smart grid". Other approaches using altered OPF formulations with intermittent generation are studied in [18] and [19], but these studies do not include energy storage.

In this paper, we consider an OPF problem with stor-

A. E. Sjödin is with the School of Engineering Sciences, KTH Royal Institute of Technology, SE-100 44 Stockholm, Sweden. emmsjo@kth.se

D. F. Gayme and U. Topcu are with the Department of Computing and Mathematical Sciences, California Institute of Technology, Pasadena, CA, USA, 91125. {dennice, utopcu}@cds.caltech.edu

age dynamics as a finite-horizon optimal control problem. Risk-limiting constraints are used to study the operational impacts of variability in generation and loads in terms of the need for spinning reserves and energy storage units. The spinning reserves are assumed to be dispatchable conventional generators, e.g. gas turbines, with short ramp up periods. Energy storage is distributed across the network and the inflow/outflow at each time is described through simple charge/discharge dynamics. We consider a case where generation from intermittent wind sources is taken to be the primary source, supplemented by these reserves and storage units. We also briefly address the problem of storage placement in networks and study how this is affected by topology and transmission constraints.

This paper is organized as follows. The next section describes the problem setup. Section III introduces the risk-limiting optimal power flow, which is studied through a series of cases studies that are outlined in Section IV. The results of these studies are then presented through the examples in Section V. Finally, we provide a summary and discuss some directions for future work.

II. PROBLEM SETUP

Consider a network with a set of buses, \mathcal{N} . The set $\mathcal{G} \subset \mathcal{N}$ of generation buses is connected by transmission links to the set $\mathcal{L} \subset \mathcal{N}$ of load buses, i.e., $\mathcal{N} = \mathcal{G} \cup \mathcal{L}$. This section describes the power flow in this network when the generation $g_k(t)$ for $k \in \mathcal{G}$ and load (demand) $d_i(t)$ for $i \in \mathcal{N}$ are given and stochastic. The problem of interest is the scheduling of ancillary services and storage over some finite time horizon T at time steps $t \in \mathcal{T} := \{0, 1, 2, \dots, T-1\}$. For simplification we use the linear DC power flow approximation, where the network's transmission links are modeled through the susceptance matrix B , where $B_{ij} = B_{ji}$ is the line susceptance between buses i and j .

A. Power Flows

The real power flow from bus i to bus j at time $t \in \mathcal{T}$ is

$$P_{ij}(t) = |V_i(t)||V_j(t)|B_{ij}\sin(\theta_i(t) - \theta_j(t)),$$

where $i, j \in \mathcal{N}$, $|V_i(t)|$, $\theta_i(t)$ are respectively the voltage magnitude and angle at bus i . This expression is simplified using the linear DC power flow approximation which assumes the voltage magnitudes at all nodes in \mathcal{N} are identically equal to the base voltage $V_o = 1$ for all $t \in \mathcal{T}$ and that the voltage angle differences are small i.e., $\sin(\theta_i(t) - \theta_j(t)) \approx \theta_i(t) - \theta_j(t)$ for all $i, j \in \mathcal{N}$. The resulting expression is

$$P_{ij}(t) = B_{ij}[\theta_i(t) - \theta_j(t)], \quad (1)$$

where by abuse of notation we use $P_{ij}(t)$ to represent the linear approximation. The small angle assumption imposed in (1) can be enforced by requiring

$$|\theta_i(t) - \theta_j(t)| \leq \Theta, \quad \text{for } i, j \in \mathcal{N} \text{ and } t \in \mathcal{T}. \quad (2)$$

The line power capacity limits \bar{p}_{ij} restrict heating of the lines and enforce network stability requirements [20] so that the

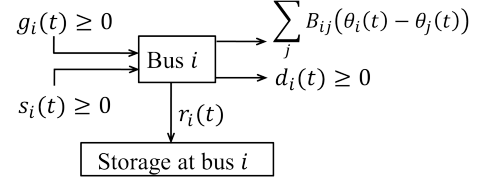


Fig. 1. The in- and out-flow of power at bus $i \in \mathcal{N}$. For $i \in \mathcal{L}$, $g_i(t) =$ and $s_i(t) = 0$, where " ≥ 0 " indicates the positive direction of the flow.

simplified power flow between nodes i and j at each $t \in \mathcal{T}$ is such that

$$|B_{ij}(\theta_i(t) - \theta_j(t))| \leq \bar{p}_{ij}, \quad \text{for } i, j \in \mathcal{N}. \quad (3)$$

Consider a system where ancillary services are provided as spinning reserves $s_k(t)$ co-located with generators $k \in \mathcal{G}$. At time $t \in \mathcal{T}$ the reserves are bounded as

$$0 \leq s_i(t) \leq S_i(t), \quad (4)$$

where $S_i(t)$ is the amount of reserves scheduled at time t , as further discussed in Section III.

If we denote the power flow into the energy storage unit located at every bus $i \in \mathcal{N}$ at time $t \in \mathcal{T}$ by $r_i(t)$, where $r_i(t)$ can either be negative (charging) or positive (discharging), then the power flow in and out of the energy storage unit at each $t \in \mathcal{T}$ is constrained as

$$R_i^{min} \leq r_i(t) \leq R_i^{max}, \quad (5)$$

where $R_i^{min} < 0$. The energy level of the storage at bus $i \in \mathcal{N}$ and each $t \in \mathcal{T}$ is then related to the charge/discharge rate through the difference equation

$$b_i(t) = b_i(t-1) + r_i(t), \quad (6)$$

with initial condition $b_i(0) = b_0 \geq 0$. The storage level is bounded by each unit's maximum capacity E_i^{max} such that

$$0 \leq b_i(0) + \sum_{\tilde{t}=0}^t r_i(\tilde{t}) \leq E_i^{max}, \quad (7)$$

for each $i \in \mathcal{N}$ and every $t \in \mathcal{T}$. We also require the energy storage level at the final time to be at least as much as at the beginning of the interval, which is captured by

$$b_i(0) \leq b_i(0) + \sum_{\tilde{t}=0}^T r_i(\tilde{t}) \leq E_i^{max}, \quad \text{for } i \in \mathcal{N}. \quad (8)$$

Figure 1 shows in- and out-flows for a bus $i \in \mathcal{N}$ at each $t \in \mathcal{T}$.

B. DC power flow approximation

The DC power (or load) flow approximation is a standard simplification of the actual power flow used to obtain a linear formulation of OPF (see e.g. [21] for derivations). The problem formulation presented herein makes use of DC power flow's three main assumptions, which are

- (i) the resistance R of each line is negligible,
- (ii) the voltage angle differences $\theta_i - \theta_j$ are small, and

(iii) the voltage variations across the network are sufficiently small to assume a flat voltage profile.

The applicability of the DC power flow model are addressed in a recent study by Purchala et al. [22]. They conclude that assumption (i) is valid for the high X/R (line reactance to resistance) ratios generally found in high voltage transmission lines [23]. The particular ratios for the IEEE 14 bus benchmark example (see [24]) that we use in the case study presented in Section IV were computed and verified to meet the criterion discussed. The authors of [22] further indicated that the small angle assumption, enabling the linearization of the trigonometric functions in the power flow equations, is also generally applicable for transmission grids. In the present work, the angles are explicitly constrained to be sufficiently small through (2). This angle constraint also limits the power transmission, which also aids in limiting voltage variations across the network to comply with assumption (iii). Clearly, use of DC power flow does not allow direct study of voltages or reactive power and the extension of this study to a full AC OPF problem is a topic of ongoing work.

C. Risk mitigation strategy

Under normal operating conditions, the total power in-flow at every bus has to match or exceed the total power out-flow at all times, i.e.,

$$g_i(t) + s_i(t) \geq d_i(t) + r_i(t) + \sum_{j \neq i} B_{ij} [\theta_i(t) - \theta_j(t)] \quad (9)$$

for $i \in \mathcal{N}$ and $t \in \mathcal{T}$. In traditional power systems reserve capacity is allocated according to the N-1 contingency criterion described earlier. This strategy ensures that the condition (9) is fulfilled even when a generator fails but this may not be the best approach in a system with a high penetration of renewables. To study such a system our risk-limiting optimal power flow problem considers an alternative risk measure, the so-called *loss-of-load probability* (LOLP). To this end, let us define the margin $M_i(t)$ between the power in-flow and the power out-flow at bus $i \in \mathcal{N}$ at time $t \in \mathcal{T}$ as

$$M_i(t) := g_i(t) + s_i(t) - \left[d_i(t) + r_i(t) + \sum_{j \neq i} B_{ij} (\theta_i(t) - \theta_j(t)) \right].$$

As discussed above, $g_i(t)$ and $d_i(t)$ are given and treated as random variables, which from an operating perspective may correspond to random wind and load forecasting errors. The probability distributions of these random variables is discussed below. Let ε_i be a given scalar which is a bound on the desired reliability level, i.e., a bound on the LOLP at bus i . Then, a probabilistic operating criterion is

$$\text{Prob} \{M_i(t) \geq 0\} \geq 1 - \varepsilon_i \quad (10)$$

for all $i \in \mathcal{N}$ and times $t \in \mathcal{T}$. Note that this probability is taken over all possible realizations of $d_i(t)$ and $g_i(t)$.

The inequality (10) is a so-called chance constraint (see e.g. [25], [26]); which is generally hard to handle and not

directly amenable to numerical optimization. Therefore, we now reformulate this constraint to a deterministic version using the theory and partly the notation given in e.g. [27].

Consider the random variable a , of which the linear transformation is constrained to be smaller than some variable b with a probability larger than η , i.e.,

$$\text{Prob} \{a^T x \leq b\} \geq \eta. \quad (11)$$

If a is normally distributed with mean μ and covariance Σ it holds that

$$\text{Prob} \{a^T x \leq b\} = \Phi \left(\frac{b - \mu^T x}{\sqrt{x^T \Sigma x}} \right).$$

We therefore have

$$\Phi \left(\frac{b - \mu^T x}{\sqrt{x^T \Sigma x}} \right) \geq \eta$$

and by rearranging we have that

$$b - \mu^T x \geq \Phi^{-1}(\eta) \|\Sigma^{1/2} x\|_2 \quad (12)$$

is an equivalent formulation to (11), in which Φ^{-1} is the inverse cumulative distribution function of the normal probability distribution and $\eta \geq 0.5$ is the confidence level.

If we assume the wind generation $g_i(t)$ and load $d_i(t)$ to be normally distributed with means and covariances $\bar{g}_i(t)$, Σ_i^G and $\bar{d}_i(t)$, Σ_i^D respectively, then

$$\mu^T(t) = -(\bar{g}_i(t) - \bar{d}_i(t)),$$

and

$$b = -r_i(t) + s_i(t) + \sum_j B_{ij} (\theta_i(t) - \theta_j(t))$$

for each bus $i \in \mathcal{N}$ and $t \in \mathcal{T}$. Finally, defining $\bar{M}_i(t) := b - \mu^T x$ allows us to apply (11) and (12) to the risk-limiting constraint (10) to obtain the following deterministic version of (10)

$$\bar{M}_i(t) \geq \Phi^{-1}(1 - \varepsilon) \|\Sigma_i^G + \Sigma_i^D\|^{1/2} \quad (13)$$

for $i \in \mathcal{N}$, $t \in \mathcal{T}$.

Remark 1: A normal distribution is a standard assumption for load prediction errors [28]. Although, statistical models for wind power outputs often use Weibull distributions [7], [29] a number of studies in the literature approximate this behavior with a Gaussian, e.g. [16] and [30].

III. RISK-LIMITING OPF

The objective of the optimization problem described herein is the scheduling of reserves and storage units while minimizing the cost of their usage over the finite time horizon \mathcal{T} , the *planning horizon*. We also assume that there is some *reserve period* $t = 0, \dots, (T_R - 1)$, $T_R < T$ for which the maximum reserve levels $S_i(t)$ at buses $i \in \mathcal{G}$ are pre-determined. Then, the optimization program determines reserve levels $S_i(t)$ for $t = T_R, \dots, T - 1$ and use $s_i(t)$ of the reserved capacity at times $t \in \mathcal{T}$, at all $i \in \mathcal{G}$ in order to ensure that the LOLP criterion is satisfied. Figure 2 illustrates the planning horizon and the reserve period.

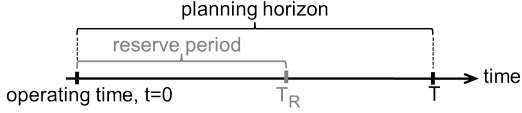


Fig. 2. The planning horizon and the reserve period at operating time $t = 0$. The reserve period is the time for which the ancillary services are pre-allocated prior to the optimization, which takes place over the full planning horizon.

Let the cost of allocating spinning reserve capacity outside the reserve period be given by

$$c_R(S) := \sum_{i \in \mathcal{G}} \sum_{t=T_R}^{T-1} H_i(S_i(t), t) \quad (14)$$

and the cost of using reserve power be

$$c_s(s) := \sum_{i \in \mathcal{G}} \sum_{t=0}^{T-1} h_i(s_i(t), t). \quad (15)$$

Additionally, we define the cost of storage use $c_B(r)$, which can be used to represent e.g. losses due to charging/discharging inefficiencies.

Given some reserve period $0 < T_R < T$, stochastic loads $d_i(t)$, renewable generation profiles $g_i(t)$, transmission capacities $\bar{p}_{ij}(t)$, initial storage levels $b_i(0)$, storage capacities E_i^{max} , storage rate limits R_i , pre-allocated reserve levels over the reserve period $S_i(0), \dots, S_i(T_R)$, and a risk level ε_i , the risk-limiting OPF problem with energy storage is

$$\min c_s(s) + c_R(S) + c_B(r) \quad (16)$$

subject to (2)–(8) and (13) over the decision variables $r_i(t), \theta_i(t)$ for $i \in \mathcal{N}$ and $t \in \mathcal{T}$, $s_i(t)$ for $i \in \mathcal{G}$ and $t \in \mathcal{T}$ - and $S_i(t)$ for $i \in \mathcal{G}$ and $t = T_R, \dots, T-1$.

A. Optimal storage placement

This framework can also be applied to investigate the optimal distribution of storage throughout the network. This requires the presented problem formulation to be slightly altered. Previously, the storage capacity E_i^{max} at each bus $i \in \mathcal{N}$ in (7) was pre-determined whereas this quantity is a decision variable in the in the optimal placement problem. In this modified formulation the total storage available constrains the sum of these decision variables, i.e.

$$\sum_{i \in \mathcal{N}} E_i^{max} \leq E^{tot}, \quad (17)$$

while the storage charge/discharge rate is still limited according to (5). This optimal storage placement problem then distributes a given amount of storage capacity with given power ratings over all of the available buses under the constraints (3) - (8), (10) and (17) while minimizing the cost function (16).

IV. CASE STUDIES

We study the risk-limited OPF problem using topology of the IEEE 14 bus benchmark system [24], which is representative of a portion of the Midwestern US transmission grid. This section describes the data sources and parameters used for the example instances of the problem that are discussed in Section V. The optimization problem was implemented numerically as a semi-definite program in MATLAB and solved for various cost functions and reserve periods using YALMIP [31].

A. Wind generation data

The IEEE 14 bus test case contains five generator buses. Generation profiles for these were created using data from five Southern Californian locations provided by the National Renewable Energy Laboratory (NREL) [32]. At each location, the data at 10 minute intervals for five individual wind turbines during July 2006 was averaged. The statistics for an average July day were then computed using the 31 days of data. The generation curves, which can be seen in Figure 3, were then scaled for the total produced energy over the 24 hour period to match the total demand, i.e. $\sum_{i \in \mathcal{N}} \sum_{t=0}^{T-1} (g_i(t) - d_i(t)) = 0$. That is, we assume the installed wind capacity is sufficient to cover the average demand. The top panel of Figure 3 shows the average generation profiles for the 5 generation buses.

B. Load data

Load profiles were created using normalized demand data from 14 typical feeders [33] for the month of July 2010. The data was interpolated to obtain points separated by ten minute intervals to match the wind generation data. Statistics were obtained by averaging of the 31 days of the month for each of the 14 load buses.

The demand curves as well as the covariances were then scaled to the IEEE 14 bus test case, letting its static demand values correspond to the peak values of the curves. The bottom panel of Figure 3 shows the resulting demand profiles for each bus.

C. Risk and uncertainty parameters

The LOLP is limited by the constraint (13). We call the right hand side as the *confidence margin* for each bus because it represents how much extra supply that is needed to produce the desired confidence level $1 - \varepsilon_i$ in (10). This depends on the assumed risk level ε and the combined covariance of generation and load. Figure 4(a) illustrates the multiplicative factor $\Phi^{-1}(1 - \varepsilon)$ in (13) as a function of ε .

Figure 4(b) illustrates confidence margin's dependence on the scalar variance given as a percentage of the nominal generation (2 p.u., representative of the total generation), with constant load variance (here set to 5% of 2 p.u.) and risk level $\varepsilon = 5\%$. Although this plot only represents an illustrative simplification of the relation used in the case studies it demonstrates how the generation variance affects the confidence margin. The covariances over time during a one day planning horizon are computed using a full month

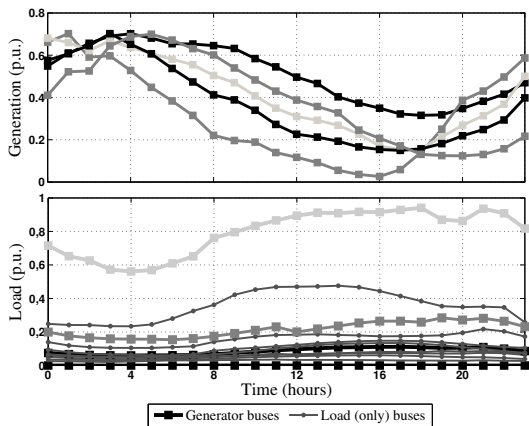


Fig. 3. Generation profiles for the five generator buses based on five Southern Californian wind farms (upper). Demand data for 14 typical feeders (lower). The data represents the generation and demand for an average day in July. These figures are plotted with hourly sub-sampling of the data.

of statistics. This procedure results in a very large standard deviation, which is partially due to the data's large intra-day fluctuations that includes days when the generators were out of use. Therefore, we reduce the variance in our data using a model based on the one suggested in [34]. Even with this modification, wind power prediction for a given planning horizon is generally more accurate than the data used herein, see e.g. [35]. The curve in Figure 4(b) shows that this overestimate of the variance means that the results obtained here will be conservative. The use of more accurate wind and load prediction models in the proposed problem formulation will be able to improve the predictions for ancillary service and storage requirements. This is a topic of ongoing research.

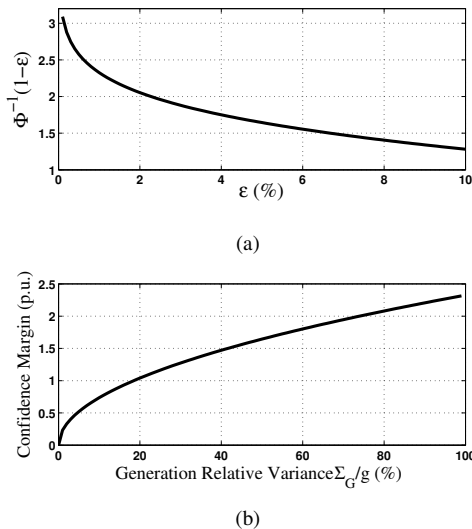


Fig. 4. (a) The multiplicative factor $\Phi^{-1}(1 - \varepsilon)$ from equation (13) as a function of the risk level ε . This function is the inverse cumulative distribution function of the normal probability distribution function and gives the size of confidence intervals at different levels. (b) The confidence margin, i.e. the right hand side of equation (13), as a function of the variance in generation relative to the nominal generation 2 p.u. with load variance = 0.1 p.u. and $\varepsilon = 5\%$

V. RESULTS AND DISCUSSION

In this section we apply the described risk-limiting OPF, (16) subject to (2)–(8) and (13), and illustrate the roles of storage units and spinning reserves in the system. We present cases with different reserve periods. Solutions to the optimal placement problem for different topologies and storage capacities are also presented. For all of the examples, we take the risk level $\varepsilon = 5\%$ and the bound in (2) to $\Theta = 10^\circ$, unless otherwise indicated.

A. Example I

We first consider the case where spinning reserves are pre-allocated for the entire planning horizon, i.e. the reserve period in Figure 2 is $T_R = T$. The spinning reserve limit is set to $S_i(t) = 1$ p.u. for all $i \in \mathcal{G}$ and $t \in \mathcal{T}$. The cost function (16) is applied using quadratic functions $H(S_i(t), t)$ and $h(s_i(t), t)$, and a linear function $c_B(r_i(t))$, with constant coefficients that are equal at all buses $i \in \mathcal{G}$. We assume the storage units have maximum charge (discharge) rates $R_i^{max} = -R_i^{min} = 0.5$ p.u. with capacity $E_i^{max} = 1.5$ p.u. for all $i \in \mathcal{N}$ for Example I and II.

Figure 5(a) illustrates the result of the risk-limited OPF. The bottom panel enables a comparison of the upper two to the total generation-load balance and illustrates the confidence margin and the fulfilment of the operating criterion (13). Here it is clear that the generation exceeds the demand until $t = 10$ h. During this time the storage charges as is seen in the center panel of Figure 5(a). Later in the day, the energy is discharged to, together with the spinning reserves, compensate for the generation deficits and the confidence margin given by the risk-limiting constraint, seen in the bottom panel of Figure 5(a).

It should be noted that the storage capacity is not fully used in this example. This is because the surplus energy in the first hours is not sufficient to fully charge the storage and compensate for the confidence margin. As expected, the storage is not charged with power generated by the spinning reserves because that would increase the cost function value.

B. Example II

In this case, we study the problem with a reserve period of 6 hours, i.e. $T_R = \frac{1}{4}T$, with pre-allocated limits of $S_i(t) = 1$ p.u. for all $i \in \mathcal{G}$ and $t = 0, \dots, T_R - 1$. The top and center panels of Figure 5(b) shows that this scenario leads to the use of the allocated spinning reserves during $t < T_R$ to fully charge the storage units. The storage units then contain enough energy to enable a minimal usage of reserves later in the day. This behavior can be explained through the nature of the cost function $c_R(s, S)$ defined in (14). This function penalizes the use of spinning reserves outside of the reserve period, when $t > T_R$. It should be noted that the spinning reserve use in the center panel of Figure 5(b) is piecewise constant, since we are using a quadratic cost function.

The use of reserve capacity during off-peak hours to charge energy storage units is reasonable from a market perspective if there is a lot of high efficiency storage available, as for example in regions where pumped storage is abundant.

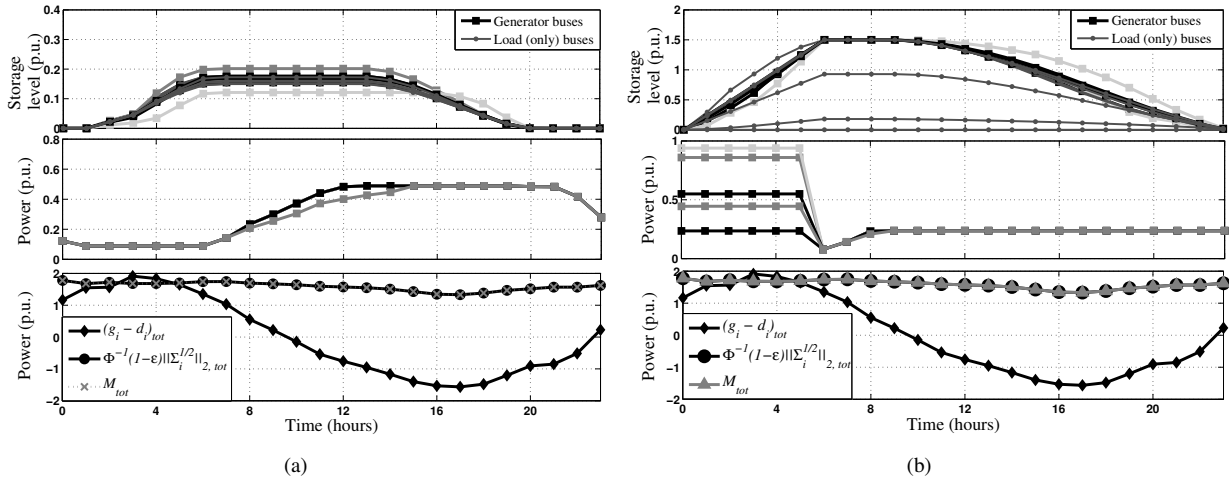


Fig. 5. Results of optimization program (a) with reserve horizon equal to the planning horizon and (b) with reserve period $T_R = 6h$. The figures show storage levels (usage) at each of the 14 buses (top) and spinning reserve usage at the five generator buses (middle) compared to the total generation-load balance and the operating criterion (bottom), where $\langle \cdot \rangle_{tot}$ denotes $\sum_{i \in \mathcal{N}} \langle \cdot \rangle$.

As mentioned in the introduction, this strategy may also be advantageous from a congestion management perspective depending on the placement of the storage. The inclusion of storage efficiencies in the formulation will better simulate the trade-off between reserves and storage and is a subject of ongoing research.

C. Optimal placement problem

To investigate the optimal placement problem introduced in Section III-A, we study simple grid topologies. This allows us to more easily isolate the effects of transmission and network constraints on the distribution of storage across the network. We expect the insights gained in this simple setting to be transferable to general network topologies. Figure 6 shows the two 4-node Y-shaped and the 3-node Δ -shaped topologies that were selected for this investigation. The properties of these networks are again modeled by the susceptance matrix B , where a low susceptance implies a long transmission line. Long lines are of particular interest as they can model the wide separation between generation and load that is expected to become important as more geographically isolated wind farms are added to the grid [36].

The generation and demand curves used in this study are sinusoids shifted by $\pi/2$, with equal loads at all buses and a generation that covers the total demand over the time period of 24 hours. Sinusoids were chosen to approximate the shapes of the real demand and generation profiles in Figure 3. The assumed uncertainty in load and generation are 30% and 50% of the peak values respectively. Figure 7(a) shows the simplified generation and load profiles in the upper panel. The lower panel of Figure 7(a) displays a characteristic storage use result, obtained for the topology in Figure 6(a) with $E^{tot} = 5$ p.u. and the voltage angle difference from (2) is set to $\Theta = 5^\circ$.

For all of the cases tested, any uneven distribution of storage over the network favored a larger share being placed on the generator bus. Therefore to describe the results in this

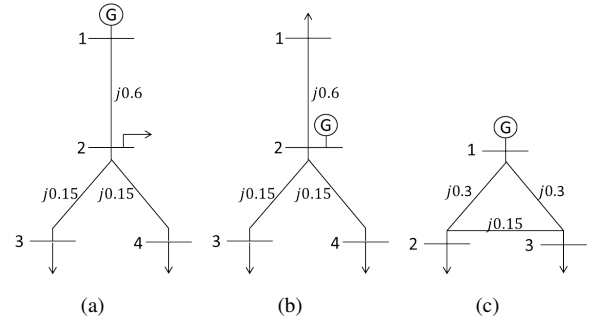


Fig. 6. Simplified topologies used to study optimal storage placement. (a) and (b) are 4-bus networks with one generator at bus 1 and 2 respectively and three load buses. (c) is a 3-bus topology with one generator at bus 1 and two symmetrically placed loads. The line impedances, in this case purely reactive, are indicated on the lines. The susceptance of the lines is the inverse of the reactance.

section we discuss the percentage by which the generator bus storage capacity exceeds the average capacity at the other buses. Figure 7(b) depicts this quantity for a number of different test settings. It shows that the advantage gained by placing more storage at the generator bus is largely a function of the power flow constraints. This dependence is illustrated by altering the angle bound Θ in (2). A larger angle $\Theta = 10^\circ$ permits a larger power flow and results in more evenly distributed storage than $\Theta = 5^\circ$, (note: both angles are well in the limits of the small angle assumption). The diagram in Figure 7(b) also illustrates the strong dependence on the total storage capacity. The topology also plays a role, for example the one in Figure 6(a) favors placing storage at the generator bus more than the other topologies that were analyzed here.

These results can be interpreted as follows. Since the DC power flow represents a lossless system, having to transmit power through the network does not have any disadvantages. Therefore when there is enough capacity, an even distribution of the storage is preferable because it can maximize the total power rate delivered by the storage units when the

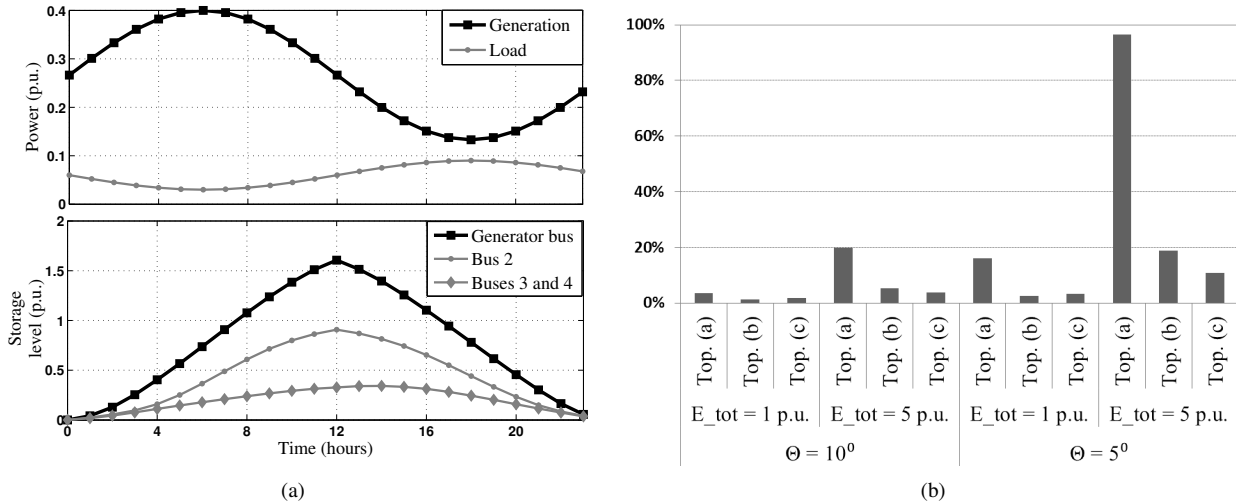


Fig. 7. (a) Simplified generation and demand schemes used to study the optimal placement problem and a typical storage usage scheme. (b) Result of placement problem for topologies given in Figure 6 given as the percentage with which the storage capacity at the generator node exceeds the capacity at the other nodes (on average), with different total capacities and power flow constraints. "Top (a)", "Top (b)" and "Top (c)" refer to the topologies of Figure 6(a)-6(c) respectively.

rate is independent of the capacity (as in the current study). However, when the transmission capacity is limited such that the peak generation can not be transmitted, it is advantageous to store the energy at the same bus as it is generated. The storage then releases the power when there is no congestion. This strategy is increasingly favored as the storage capacity and isolation (distance from the other nodes) of the generator bus is increased, as illustrated by the results for topology (a), which has the longest distance to the load buses. The corresponding topology (b), but with the generator at bus 2, enables transmission of power through more than one line and less storage is needed at the generator. For these reasons, buses with very high loads and highly interconnected nodes may also be strategic for storage placement.

VI. SUMMARY AND POTENTIAL EXTENSIONS

We have formulated an optimal power flow problem with risk-limiting constraints to study the scheduling of spinning reserves and energy storage as a finite-horizon optimal control problem. Our formulation models the pre-allocation of spinning reserves for a portion of the planning (optimization) horizon.

A natural extension of this work would be a receding horizon implementation, where the pre-allocation for some reserve period is determined at each update. This type of implementation would also benefit from some data forecasting technique for both wind levels and demand. Such a framework may be useful in studying different market strategies for pre-allocation of ancillary services. For example, day-ahead versus hour-ahead markets could be compared through changing the reserve period described in Figure 2.

We investigated the effects of wind and load variability on the scheduling of spinning reserves and storage units on the IEEE 14 bus benchmark system. We modeled an extreme case with wind as the primary energy source and compensate

for the variability using reserves that are allocated based on probabilistic operating criteria. The reserve requirements computed in our study represent a worst-case scenario because there is no wind or load forecasting included in our model. The inclusion of an accurate model of wind prediction and its errors are topics of ongoing study as is the inclusion of time correlations for the wind and load data.

Two important next steps are the extension of this framework to an AC power flow setting and the introduction of storage efficiencies, which would allow cost benefit analysis of different storage technologies. Both of these extensions would be beneficial in the storage placement problem that was introduced here. Our results for that problem demonstrated the dependence of the storage placement on transmission line limits and network congestion. In the lossless DC power flow model co-locating storage with wind thus seems to be a preferable strategy. Although, the authors of [8] also advocate co-locating wind and storage for the sake of increased transmission capacity, they indicate that the value of the storage as an ancillary services provider is higher when co-located with the loads. Investigation of such a scenario would be better carried out in an AC setting where transmission losses and voltage drop can be included in the analysis. The extension of the placement problem to the AC framework is part of our ongoing research.

VII. ACKNOWLEDGEMENTS

The authors acknowledge the support of NSF through grant CNS-0911041, Southern California Edison (SCE) and the Boeing Corporation. A special thank you to Christopher Clarke of Southern California Edison for providing some of the data used in this work. We are also grateful to Steven Low and K. Mani Chandy of the California Institute of Technology for their insightful comments and a number of interesting discussions.

REFERENCES

- [1] G. Boyle, Ed., *Renewable Energy: Power for a Sustainable Future*, 2nd ed. Oxford University Press, 2004.
- [2] U.S. Energy Information Administration, "Annual energy outlooks 2010 with projections to 2035," U.S. Department of Energy, Tech. Rep. DOE/EIA-0383, 2010. [Online]. Available: <http://www.eia.doe.gov/oiaf/aeo>
- [3] F. van Hulle, "Large scale integration of wind energy in the european power supply: analysis, issues and recommendations," EWEA, The European Wind Energy Association, Tech. Rep., 2005.
- [4] P. Varaiya, F. Wu, and J. Bialek, "Smart operation of smart grid: Risk-limiting dispatch," *Proc. of the IEEE*, vol. 99, no. 1, pp. 40–57, Jan. 2011.
- [5] Y. M. Atwa and E. F. El-Saadany, "Optimal allocation of ESS in distribution systems with a high penetration of wind energy," *IEEE Trans. on Power Systems*, vol. 25, no. 4, pp. 1815–1822, Nov. 2010.
- [6] B. Robyns, J. Sprooten, and A. Vergnol, "Supervision of renewable energy for its integration in the electrical system," in *Proc. of IEEE PES General Meeting*, July 2010, pp. 1–8.
- [7] J. P. Barton and D. G. Infield, "Energy storage and its use with intermittent renewable energy," *IEEE Trans. on Energy Conversion*, vol. 19, no. 2, pp. 441–448, 2004.
- [8] P. Denholm and R. Sioshansi, "The value of compressed air energy storage with wind in transmission-constrained electric power systems," *Energy Policy*, vol. 37, no. 8, pp. 3149–3158, 2009.
- [9] T. Yau, L. Walker, H. Graham, and A. Gupta, "Effects of battery storage devices on power system dispatch," *IEEE Trans. on Power Apparatus and Systems*, vol. PAS-100, no. 1, pp. 375–383, 1981.
- [10] N. Alguacil and A. J. Conejo, "Multi-period optimal power flow using benders decomposition," *IEEE Trans. Power Systems*, vol. 15, no. 1, pp. 196–201, 2000.
- [11] M. Geidl and G. Andersson, "A modeling and optimization approach for multiple energy carrier power flow," in *Proc. of IEEE PES PowerTech*, 2005.
- [12] E. Sortomme and M. A. El-Sharkawi, "Optimal power flow for a system of microgrids with controllable loads and battery storage," in *Power Systems Conf. and Exposition*, 2009.
- [13] F. Kienzle and G. Andersson, "Location-dependent valuation of energy hubs with storage in multi-carrier energy systems," in *7th Int'l Conf. on the European Energy Market (EEM)*, June 2010, pp. 1–6.
- [14] P. Meibom, R. Barth, B. Hasche, H. Brand, C. Weber, and M. O'Malley, "Stochastic optimization model to study the operational impacts of high wind penetrations in Ireland," *IEEE Trans. on Power Systems*, vol. 26, no. 3, pp. 1367–1379, Aug. 2011.
- [15] J. Restrepo and F. Galiana, "Effects of wind power on day-ahead reserve schedule," in *Proc. of IEEE PES/IAS Conf. on Sustainable Alternative Energy (SAE)*, Sept. 2009, pp. 1–4.
- [16] F. Bouffard and F. D. Galiana, "An electricity market with a probabilistic spinning reserve criterion," *IEEE Trans. on Power Systems*, vol. 19, no. 1, pp. 300–307, 2004.
- [17] —, "Stochastic security for operations planning with significant wind power generation," in *Proc. of IEEE PES General Meeting*, 2008.
- [18] R. Jabr, "Optimal Power Flow Using an Extended Conic Quadratic Formulation," *IEEE Trans. on Power Systems*, vol. 23, no. 3, pp. 1000–1008, Aug. 2008.
- [19] H. Ahmadi and H. Ghasemi, "Probabilistic optimal power flow incorporating wind power using point estimate methods," in *Proc. of the 10th Int'l Conf. on Environment and Electrical Eng. (EEEIC)*, May 2011, pp. 1–5.
- [20] A. R. Bergen and V. Vittal, *Power Systems Analysis*, 2nd ed. Prentice Hall, 2000.
- [21] X.-F. Wang, Y. Song, and M. Irving, *Modern Power Systems Analysis*, 1st ed. Springer Science+Business Media, 2008.
- [22] K. Purchala, L. Meeus, D. Van Dommelen, and R. Belmans, "Usefulness of DC power flow for active power flow analysis," in *Proc. of IEEE PES General Meeting*. IEEE, 2005, pp. 2457–2462.
- [23] H. Saadat, *Power System Analysis*, 3rd ed. PSA Publishings, 2010.
- [24] University of Washington, "Power systems test case archive." [Online]. Available: <http://www.ee.washington.edu/research/pstca/>
- [25] D. Bertsimas and M. Sim, "Tractable approximations to robust conic optimization problems," *Mathematical Programming*, vol. 107, pp. 5–36, 2006.
- [26] A. Charnes and W. W. Cooper, "Chance-constrained programming," *Management Science*, vol. 6, no. 1, Oct.
- [27] S. Boyd and L. Vandenberghe, *Convex Optimization*. Cambridge Univ. Press, 2004.
- [28] G. Gross and F. D. Galiana, "Short-term load forecasting," *Proc. of the IEEE*, vol. 75, no. 12, pp. 1558–1573, 1987.
- [29] R. Jabr and B. Pal, "Intermittent wind generation in optimal power flow dispatching," *IET Generation, Transmission & Distribution*, vol. 3, no. 1, pp. 66–74, Jan. 2009.
- [30] L. Söder, "Reserve margin planning in a wind-hydro-thermal power system," *IEEE Trans. on Power Systems*, vol. 8, no. 2, pp. 564–571, May 1993.
- [31] J. Löfberg, "YALMIP : A toolbox for modeling and optimization in MATLAB," in *Proc. of the CACSD Conf.*, Taipei, Taiwan, 2004. [Online]. Available: <http://control.ee.ethz.ch/~joloef/yalmip.php>
- [32] Y. Jiang, K. Kudryavtseva, J. Marinova, and S. Narayan, "Western Wind and Solar Integration Study," Tech. Rep., 2005, subcontract report NREL/SR-550-47434. [Online]. Available: <http://www.osti.gov/bridge/>
- [33] Personal communication with researchers from Southern California Edison.
- [34] A. Fabbri, T. Gomez San Roman, J. Rivier Abbad, and V. Mendez Quezada, "Assessment of the cost associated with wind generation prediction errors in a liberalized electricity market," *IEEE Trans. on Power Systems*, vol. 20, no. 3, pp. 1440–1446, Aug. 2005.
- [35] G. Sideratos and N. Hatzigiorgiou, "An advanced statistical method for wind power forecasting," *IEEE Trans. on Power Systems*, vol. 22, no. 1, pp. 258–265, Feb. 2007.
- [36] A. Mills, R. Wiser, and K. Porter, "The Cost of Transmission for Wind Energy: A Review of Transmission Planning Studies," Tech. Rep., 2009, US Department of Energy Contract No. DE-AC02-05CH11231. [Online]. Available: <http://eetd.lbl.gov/EA/EMP/>